In Situ FT−IR Study on the Effect of Cobalt Precursors on CO Adsorption Behavior†

ARTICLE *in* THE JOURNAL OF PHYSICAL CHEMISTRY C · SEPTEMBER 2010

Impact Factor: 4.77 · DOI: 10.1021/jp104878e

In Situ FT-IR Study on the Effect of Cobalt Precursors on CO Adsorption Behavior†

Nitin Kumar,‡ K. Jothimurugesan,|| George G. Stanley,§ Viviane Schwartz,⊥ and J. J. Spivey*,‡

Department of Chemical Engineering and Department of Chemistry, Louisiana State University, Baton Rouge, Louisiana 70803, Chevron Energy Technology Company, 100 Chevron Way, 10-2422, Richmond, California 94801, Center for Nanophase Material Sciences, Oak Ridge National Laboratory, Oak Ridge Tennessee 37831

Received: May 27, 2010; Revised Manuscript Received: August 6, 2010

Cobalt−rhenium based catalysts were prepared by coimpregnation from two different cobalt precursors: cobalt nitrate [CoRe(N)] and cobalt acetate [CoRe(A)]. They were characterized by H_2-TPR, ICP, XRD, DRIFTS, and activity/selectivity in CO hydrogenation. The results showed that precursors have a significant effect on the cluster size, dispersion, and CO adsorption/CO hydrogenation activities. XRD showed no bulk crystallinity for the CoRe(A) catalyst, whereas peaks corresponding to a Co_3O_4 phase were found for the CoRe(N) catalyst. TPR results suggested greater cobalt−rhenium contact for the CoRe(A) catalyst, with Re facilitating reduction of cobalt oxide by hydrogen spillover. Activity/selectivity studies showed that the CoRe(N) catalyst is more active for CO hydrogenation with high selectivity toward hydrocarbons, while the CoRe(A) catalyst has far higher selectivity to oxygenates (but considerably lower overall activity). DRIFTS studies at 25 °C for CO reacting with CoRe(N) showed lower frequency carbonyl bands (2057 and 1942 cm^{-1}), whereas CoRe(A) had CO bands at much higher frequencies (2183−2175, 2125, and 2074 cm^{-1}). The carbonyl bands in the 2183−2175 cm^{-1} region are assigned to Co(II)/Co(III)−CO from the presence of nonreduced Co_3O_4 on the surface of the CoRe(A) catalyst. DRIFTS studies under CO hydrogenation conditions are also presented. Lower wavenumber IR bands seen between 1990 and 1920 cm^{-1} for CoRe(N) are tentatively assigned to bridging CO's on the cobalt and terminal carbonyls on Re(0) clusters. Only higher frequency CO's are observed for CoRe(A) corresponding to less electron-rich cobalt centers, linear CO coordination, and oxygenate production. The presence of nanoparticle catalysts and highly dispersed Re on the CoRe(A) catalyst is proposed to be key factors in the high oxygenate selectivity. CO is weakly adsorbed on these sites facilitating the M−CO bond dissociation and increasing the CO insertion probability leading to the oxygenate formation.

Introduction

The increasing demand for clean fuel has led to increased research interest in the production of liquid fuels from sources other than petroleum. The conversion of coal- or biomass-derived syngas to ethanol is a promising alternative.[2−5] Cobalt-based catalysts have been found to be advantageous for the conversion of syngas to liquid fuels because of their low costs, low water−gas shift activity, and high activity for CO hydrogenation.[6−8]

Carbon monoxide adsorption and hydrogenation on supported cobalt catalysts has been studied extensively, e.g., where CO is used as probe to identify the nature of adsorption sites.[9−11] An understanding of this adsorption/hydrogenation process at the molecular level is important in order to understand the syngas reactions on various supported metal catalysts. Diffuse reflectance infrared Fourier transform spectroscopy (DRIFTS) can be used to probe the active sites, adsorbed species, and intermediates on the catalyst surface. Song et al.[12] used this technique to study CO adsorbed on Co/SiO_2 catalysts with different pore sizes and found different CO adsorption sites which changed with changing pore sizes. They also observed that the intensities of linear and bridge-type CO adsorption changed significantly with pore size. Heal et al.[13] used IR to study CO adsorbed on Co/SiO_2 at different temperatures and correlated the observed shift in spectra to the change in bond strength of C−O adsorbed on the surface, which is influenced by the C-metal bond strength. They also attributed methane formation to linearly adsorbed CO.

Addition of Re to Co/SiO_2 catalysts has been found to improve selectivity toward oxygenates, especially ethanol.[14] Re has been found to promote activation of the cobalt site in the catalyst via reduction of oxidized cobalt species to the metallic state and keeping the cobalt highly dispersed.[14−16] Small amounts of Re have been found to significantly increase the amount of adsorbed CO on cobalt and thus CO hydrogenation rates.[16]

Zirconia has been proposed as an important promoter for Co/SiO_2 catalysts.[17] Addition of ZrO_2 promoter can modify and improve the catalyst texture and porosity, assist in the reduction of oxidized Co species to metallic cobalt,[18,19] increase the dispersion of cobalt, and improve the chemical stability of the support.[20] Preimpregnated zirconia is believed to form a protecting layer to prevent the reaction between silica and cobalt to form inert cobalt silicates.[17,20]

Cobalt precursors have a significant effect on the activity of catalysts and product distribution, and their role has been investigated by several researchers.[14,21,22] One study showed a higher total catalytic activity when using a cobalt nitrate precursor relative to a cobalt acetate precursor.[14] It is important to understand the surface phenomenon in order to explain this precursor effect.

† Part of the "Alfons Baiker Festschrift".
* To whom correspondence should be addressed.
‡ Department of Chemical Engineering, Louisiana State University.
§ Department of Chemistry, Louisiana State University.
|| Chevron Energy Technology Company.
⊥ Oak Ridge National Laboratory.

10.1021/jp104878e
Published on Web 09/03/2010

The objective of the work reported here is to investigate different active sites for cobalt catalysts prepared from acetate and nitrate precursors and to correlate those sites with CO adsorption/hydrogenation activity in order to understand the reaction mechanism on these catalysts, particularly the formation of oxygenates.

Experimental Section

Catalyst Preparation. Co−Re/SiO_2 based catalysts were synthesized using a conventional incipient wetness impregnation method. Cobalt−rhenium catalysts prepared from cobalt nitrate and cobalt acetate precursors (designated as CoRe(N) and CoRe(A) respectively) were prepared using a SiO_2 support obtained from Alfa Aesar (surface area = 300 m^2/g, pore volume = 1 cc/g) which was modified with 2% Zr by impregnation. Zirconium(IV) oxynitrate hydrate, $ZrO(NO_3)_2 \cdot 6H_2O$, was used as the Zr precursor. The modified support was dried for 2 h at 120 °C and calcined in air for 2 h at 500 °C. A mixture of cobalt and rhenium salts was simultaneously impregnated on the Zr-modified support. Perrhenic acid, $Re_2O_7(OH)_2$, was used as the Re precursor, cobalt(II) nitrate hexahydrate, $Co(NO_3)_2 \cdot 6H_2O$, and cobalt(II) acetate tetrahydrate, $Co(CH_3COO)_2 \cdot 4H_2O$, were used as cobalt precursors. The catalyst was dried for 2 h at 120 °C and calcined under air flow for 2 h at 300 °C at a ramp rate of 1 °C/min. Both catalysts contain 10 wt % cobalt (as metal Co) and 4 wt % Re.

Temperature Programmed Reduction (TPR). Temperature programmed reduction (TPR) profiles of the calcined catalysts were recorded using Altamira AMI 200-R-HP unit equipped with a thermal conductivity detector (TCD). The catalyst samples were first purged in a fixed bed micro reactor system under flowing argon at 150 °C for 1 h to remove traces of water and then cooled to 25 °C. TPRs were performed using a 10% H_2/Ar mixture at a flow rate of 50 cm^3/min while the temperature was linearly ramped from 25 to 750 °C using a ramp rate of 10 °C/min.

X-ray Diffraction (XRD). XRD measurements were carried out with Bruker/Siemens D5000 automated powder X-ray diffractometer using Cu Kα radiation (λ = 1.5406 Å). Fresh calcined catalysts were used for the XRD measurements.

Inductively Coupled Plasma-Optical Emission Spectrometry (ICP-OES). The trace element determinations were performed on a Varian Vista AX CCD Simultaneous ICP-OES. Varian ICPExpert version 4.0 was used by ICP-OES.

Catalyst Activity Test. CO hydrogenation reactions at differential conversions were carried out in a 1/4″ glass-lined stainless steel fixed bed microreactor system at different temperatures (230 and 270 °C) and total pressure of 10 bar. Prior to reaction, the catalyst was reduced in situ for 4 h at 400 °C in flowing H_2/He mixture (50% H_2). CO hydrogenation reactions were carried out with a H_2:CO ratio of 2:1. For these experiments the syngas was diluted with helium to reduce heat effects within the bed and to ensure that the conversion was low enough to keep the oxygenated products in the vapor state for online GC/MS analysis. The GC/MS system used for the outlet product gas analysis (Agilent Technologies 6890N/5975B) is equipped with two thermal conductivity detectors (TCD). The line from the reactor exit to the sampling valve is heat traced to prevent products from condensing upstream of the GC/MS. The sampling valves are placed in an isothermal oven and maintained at a temperature of 250 °C. Oxygenates and C_2−C_4 hydrocarbons analysis were done using the mass selective detector (MSD), whereas CO, H_2, and CH_4 were analyzed on the TCD. All selectivities are reported in terms of carbon efficiency defined as:

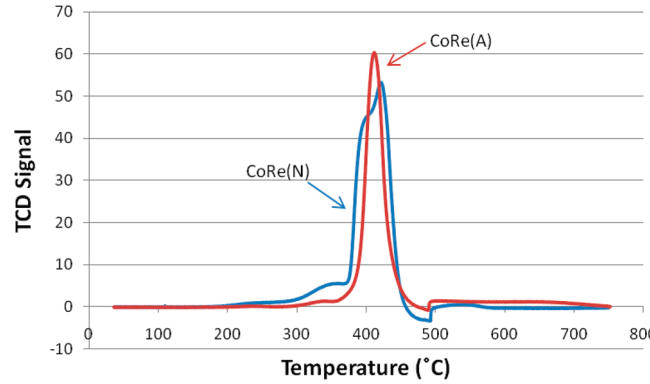

Figure 1. Temperature programmed reduction of CoRe(N) and CoRe(A).

$$\text{selectivity of A}(\%) = \frac{n(C_n)_A}{\text{total CO reacted}} \times 100$$

where n is the number of carbons in A and $(C_n)_A$ is mol fraction of A.

In Situ Diffuse Reflectance FTIR Spectroscopy (DRIFTS). FTIR spectra were collected with a Nexus 870 model (Thermo Nicolet) spectrometer equipped with a MCT-A detector cooled by liquid nitrogen. KBr beamsplitter was used to obtain spectra in the range of 4000−650 cm^{-1}. In situ measurements were carried out in a ceramic sample holder equipped with a thermocouple. Provisions were made to the cell for gas inlet, outlet, heating, and cooling. A sample holder was used to hold ∼20 mg of catalyst. DRIFTS spectra were collected by using series collection for 15 min. For each spectrum 32 scans at a resolution of 4 cm^{-1} were used.

Before each experiment the catalyst was heated in helium at 150 °C for 30 min to remove any moisture and gases. The catalyst was reduced by flowing a mixture of hydrogen and helium (4% H_2 in He) for 2 h at 350 °C. The cell was then flushed with helium and temperature was brought back to 25 °C. Backgrounds were collected at desired temperatures (270, 230, and 25 °C) during the cooling process after the system is allowed to equilibrate for 15 min at that temperature. Difference spectra were obtained by subtracting the background from the subsequent spectra. Two series of experiments were performed at each temperature: CO adsorption and CO hydrogenation. Each series was set for 15 min and was divided into three parts. In the first part helium was flowed for 20 s followed by flowing CO + He for 7 min in the second part. The third part consisted of flushing with helium (for CO adsorption studies) or flowing H_2 + He (for CO hydrogenation studies) for the rest of the time. 2% CO/2% Ar/He was used for CO adsorption/hydrogenation. The experiments were carried out at 25, 230, and 270 °C and performed at atmospheric pressure.

Results and Discussion

Temperature Programmed Reduction (TPR). TPR results in Figure 1 show a small peak at around 335 °C on both catalysts due to reduction of large crystalline Co_3O_4.[23] This peak is very small in case of CoRe(A), indicating that only a small amount of large crystalline Co_3O_4 is present. The shoulder peak found in CoRe(N) at around 400 °C is due to the reduction of rhenium oxide.[24] The reduced Re promotes the reduction of cobalt by

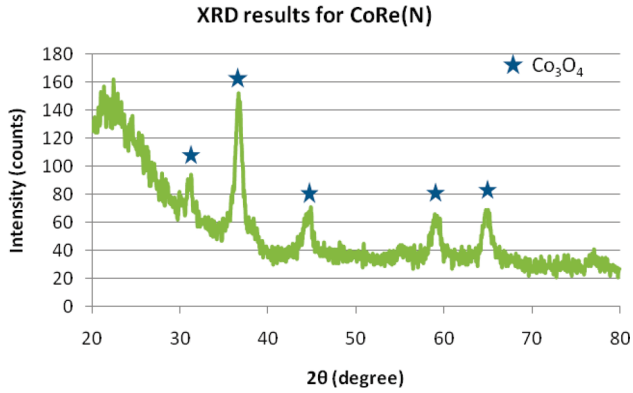

Figure 2. XRD for catalyst CoRe(N).

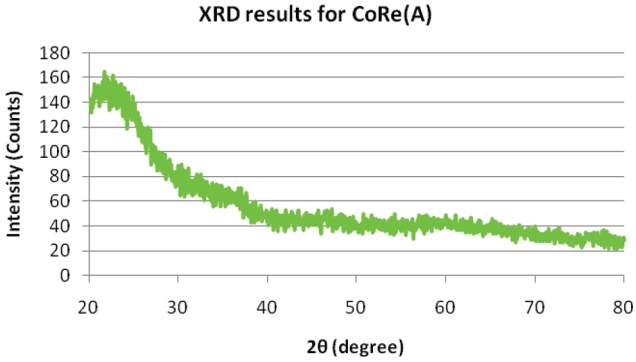

Figure 3. XRD for catalyst CoRe(A).

hydrogen spillover from Re to cobalt oxide.[14,24] The peak at around 415 °C on both catalysts is due to the reduction of highly dispersed cobalt oxide.[24] For CoRe(A), the peak due to reduction of this dispersed cobalt oxide phase overlaps with the peak due to reduction of rhenium oxide at around 405 °C. The fact that both rhenium and highly dispersed cobalt reduce at same temperature suggests that Re is in the immediate vicinity of cobalt, facilitating its reduction by hydrogen spillover.[14,25]

X-ray Diffraction (XRD). The XRD results for CoRe(N) and CoRe(A) are shown in Figures 2 and 3, respectively. No XRD peaks were observed for CoRe(A), indicating that any cobalt crystallites are less than ~2 nm, in agreement with the results reported by Matsuzaki et al.[14] for a 5% Co to 5% Re/SiO_2 catalyst prepared from cobalt acetate precursor. Matsuzaki et al.[14] reported observing a diffraction pattern for rhenium metal in their XRD, but the XRD pattern was not provided. The only obvious difference, other than slightly higher Re loading compared to our catalysts (5% vs 4%) is the fact that they used ammonium perrhenate (NH_4ReO_4) as the Re precursor, while we used perrhenic acid, $Re_2O_7(OH_2)_2$. The absence of a Re peak for both the catalysts indicate that Re is highly dispersed. The fact that we do not see any Co_3O_4 phase peaks in XRD for CoRe(A) also indicates that cobalt clusters are also highly dispersed after modification with Re. The CoRe(N) catalyst gives peaks corresponding to a crystalline Co_3O_4 phase. This result is in agreement with Matsuzaki et al.[14] for an unpromoted 5% Co/SiO_2 catalyst and Martinez et al.,[26] who reported a crystalline Co_3O_4 phase for 1% Re/20% Co/SBA-15 prepared from a cobalt nitrate precursor.

ICP-OES. The results for ICP-OES are presented in Table 1. The figures indicate metal wt %. The metal loadings are close to their intended values. There is a small, but statistically significant difference in Co and Re contents.

Catalyst Activity Tests. The results of CO hydrogenation tests for CoRe(N) and CoRe(A) are presented in Table 2.

TABLE 1: ICP Metal Analysis Results for Catalysts CoRe(N) and CoRe(A)[a]

catalyst	Co	Re	Zr
CoRe(N)	9.37	4.88	1.93
CoRe(A)	8.65	4.70	1.89

[a] Errors in reported values are within ±1%.

TABLE 2: Selectivities of Products of CO Hydrogenation Reaction at Different Temperatures for CoRe(N) and CoRe(A)[a]

catalyst	temp (°C)	EtOH %	MeOH %	CH_4 %	C_{2+} Oxy %[b]	C_{2+} HC %[c]	CO conversion (%)
CoRe(N)	230	3.0	1.4	39.5	3.6	47.8	4.1
CoRe(A)	230	15.9	5.7	45.2	1.3	23.5	0.3
CoRe(N)	270	0.4	0.3	45.9	2.1	42.0	29.4
CoRe(A)	270	15.9	7.8	34.2	5.2	29.3	3.7
CoRe(N)	300	0.1	0.1	46.8	1.1	32.2	47.0
CoRe(A)	300	9.5	3.2	43.5	2.8	33.9	10.2

[a] Pressure = 10 bar, $2H_2/CO$, catalyst wt = 50 mg, space velocity = 72 000 scc h^{-1} g cat^{-1}. [b] Includes higher oxygenates other than methanol and ethanol. [c] Includes higher hydrocarbons other than methane.

These results show that CoRe(N) is more active for CO hydrogenation (indicated by the higher CO conversion) compared to CoRe(A). The results discussed in the in situ DRIFTS section gives some insight about the differences in activity. It is interesting to see that, even in the case of similar CO conversion (e.g., compare CoRe(N) at 230 °C to CoRe(A) at 270 °C), the CoRe(A) catalyst produces less methane, even though the higher temperature should lead to higher methane selectivity. However, the selectivity toward oxygenates is much greater for CoRe(A) as compared to CoRe(N) at all temperatures. For example, the ethanol selectivity at 270 °C is 15.9% for CoRe(A) versus 0.4% for CoRe(N). This can be attributed to the presence of highly dispersed cobalt with very small crystallite size for CoRe(A), as suggested by XRD results. A similar effect of metal cluster size on oxygenates selectivity for Pd/SiO_2 catalysts has been reported[27] where increased selectivities toward oxygenates are attributed to smaller Pd cluster sizes in the range 5−19 nm. Also, the presence of Re in close proximity to cobalt for CoRe(A), suggested by the TPR results, also increases oxygenates selectivity. This result is in agreement with Matsuzaki et al.,[14] who found that a Co−Re/SiO_2 catalyst prepared from cobalt acetate precursor had a far greater ethanol selectivity than a nominally identical catalyst prepared from cobalt nitrate precursor. They attribute the increase in ethanol/oxygenates selectivity to the presence of small cobalt clusters that are more easily reduced by hydrogen spillover from rhenium. Comparison of our results on the CoRe(N) and CoRe(A) catalysts show a similar trend - higher ethanol/oxygenates selectivity for CoRe(A), which we also attribute to the smaller cobalt cluster size on the CoRe(A) catalyst. Further, our results show that hydrocarbon formation on CoRe(A) is suppressed as compared to CoRe(N), in agreement with Matsuzaki et al.[14]

In Situ DRIFTS: CO Adsorption at 25 °C. The DRIFTS spectra of the carbonyl region for CoRe(A) as a function of time are shown in Figure 4. These spectra were taken after the catalyst was reduced in situ with H_2. The peak observed at 2059 cm^{-1} during the start of CO flow can be assigned to linearly coordinated CO to a Co(0) center on the surface of the catalyst.[1] This peak shifts to higher wavenumbers (2059 cm^{-1} → 2079

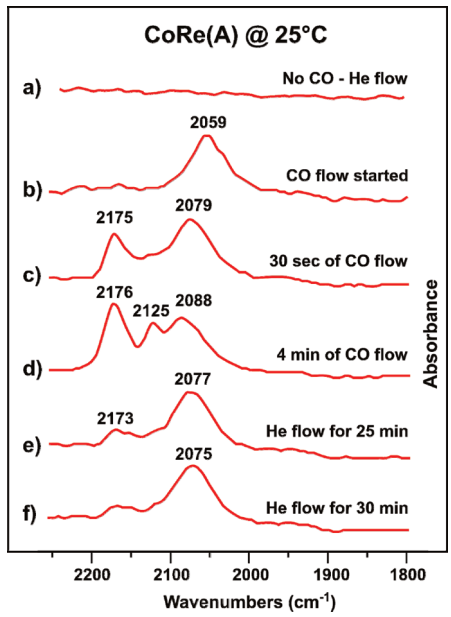

Figure 4. FT-IR spectra for CO adsorption at 25 °C and 1 atm pressure for CoRe(A) catalyst.

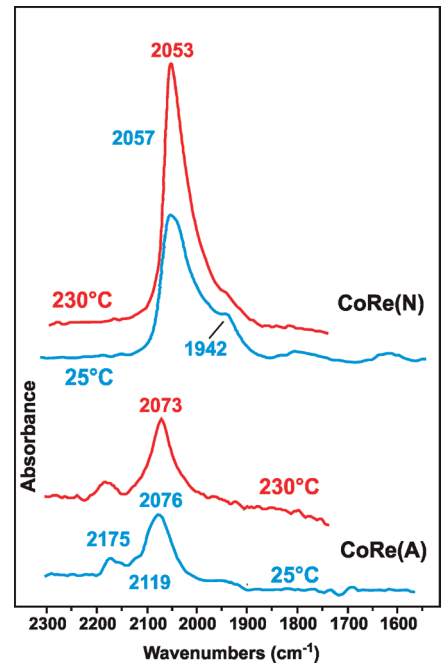

Figure 5. FT-IR spectra for CO adsorption at 25 and 230 °C at 1 atm for catalysts CoRe(N) and CoRe(A) after helium flushing for 7 min.

$cm^{-1} \rightarrow 2088\ cm^{-1}$) with time reflecting a decrease in π-backbonding from the Co atoms to the carbonyl ligands. As more CO coordinates to the surface there are fewer cobalt atoms without electron-withdrawing CO ligands that can donate electron-density to nearby cobalt atoms that have CO's coordinated. The increase in electron-withdrawing π-backbonding carbonyls causes a general decrease in surface electron-density resulting in the steady shift to higher CO stretching frequencies and weaker cobalt−carbonyl bonding.

The peak at 2176 cm^{-1} is higher than that for free CO (2143 cm^{-1}) indicating that there is no π-backbonding taking place between the metal center and carbonyl ligand. When CO acts as a simple σ-donor, the carbonyl stretching frequency increases above 2143 cm^{-1}. This points to CO coordinating to higher oxidation state Co(II)/Co(III) centers, probably from Co_3O_4 nanoclusters formed during calcining that were not fully reduced upon subsequent H_2 treatment. Busca and co-workers[28] studied the coordination of CO to Co_3O_4 and found a relatively strong carbonyl band near 2180 cm^{-1}. They also found that CO rapidly reduces Co_3O_4 to form Co(II) and Co(I) oxidation state centers at room temperature.

The peak that grows in at 2125 cm^{-1} can most likely be assigned to CO coordinated to Co(I) centers generated from the CO-induced reduction of Co_3O_4. Busca also observed this as the appearance of a CO band at 2120 cm^{-1}.[28] It can be seen from the CO band growth pattern that CO preferentially coordinates to the most electron-rich Co(0) sites in a linear fashion at the beginning of CO flow (peak at 2059 cm^{-1}). Coordination to higher oxidation state Co(II)/Co(III) centers initially produces the 2176 cm^{-1} band, followed almost immediately by CO-induced reduction of some of the Co(II)/Co(III) centers to Co(I) leading to growth of the Co(I)−CO species at 2125 cm^{-1}.

When the CO flow is stopped and helium flow started, the more weakly coordinated CO ligands with the 2176 and 2125 cm^{-1} bands are preferentially removed causing those bands to decrease in intensity first, but some of the CO coordinated to Co(II)/Co(III) and Co(I) remains even after flushing with helium for 30 min. The persistence of these higher wavenumber bands indicates nanoporous Co_3O_4 where some of the coordinated CO is partially protected in nanocracks or holes and not as easily lost as one would expect for a simple surface bound CO with such a high stretching frequency.

A comparison of CO adsorption at 25 °C between catalysts CoRe(N) and CoRe(A) after 7 min of helium flushing is shown in Figure 5. No Co(II)/Co(III)−CO (~2175 cm^{-1}) or Co(I)−CO (2119 cm^{-1}) bands are observed for CoRe(N). The peak at 2057 cm^{-1}, as with CoRe(A), is due to linearly adsorbed CO to a Co(0) center. This lower stretching frequency points to more electron-rich cobalt centers relative to the CoRe(A) catalyst system where a 2076 cm^{-1} value is seen.

The 1942 cm^{-1} shoulder on CoRe(N) can either be assigned to a bridged metal carbonyl (M_2−CO)[29] or to a terminal carbonyl on an even more electron-rich metal center. There is considerable disagreement in the heterogeneous surface literature about what CO stretching frequencies indicate bridging CO's. A majority of authors cite values below 2000 cm^{-1} as indicating bridging CO's, with values below 1900−1850 cm^{-1} indicating triply bridging CO's.[8,9,12,13,30−33]

Molecular carbonyls, sometimes referred to as polycarbonyls in the heterogeneous literature, point to a very different story with doubly bridging CO's for cobalt complexes having frequencies, for example, between 1720 cm^{-1} for $Co_2(\mu\text{-}CO)_2(CO)_2$-(et,ph-P4), where et,ph-P4 = $(Et_2PCH_2CH_2)(Ph)PCH_2P(Ph)$-$(CH_2CH_2PEt_2)$, a strongly donating tetraphosphine ligand,[34] to 1866 cm^{-1} for $Co_2(\mu\text{-}CO)_2(CO)_6$.[35] Triply bridging carbonyls in molecular $Co_2M(\eta^5\text{-}Cp^*)_2(\mu\text{-}CO)_3(\mu_3\text{-}CO)$ {M = $Cr(\eta^6\text{-}C_6H_5Me)$, $Mn(\eta^5\text{-}C_5H_4Me)$, $Fe(\eta^4\text{-}C_4H_4)$, $Fe(CO)_3$, and $Co(\eta^5\text{-}C_5H_4Me)$} complexes lie even lower in the 1622−1693 cm^{-1} range.[36]

Perhaps influenced by CO stretching frequencies in well-characterized molecular complexes, there is a smaller camp of authors that generally limit assignments of bridging carbonyls to bands below 1900 cm^{-1} and down to about 1750 cm^{-1}, although triply bridging carbonyl assignments often start appearing at the lower end of this wavenumber regime.[1,9,37] DFT calculations also support the assignment of terminal CO bands down into the upper 1800 cm^{-1} region, depending on the nature

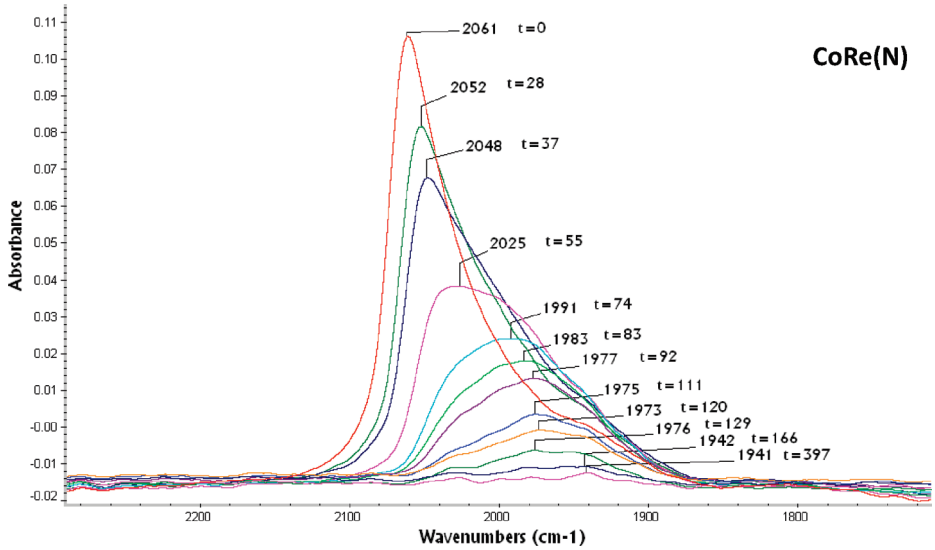

Figure 6. FT-IR spectra for CO hydrogenation at 230 °C and 1 atm for CoRe(N) at different times (in seconds) after starting H_2 flow ($t = 0$ corresponds to when H_2 flow started).

of the metal atom to which it is coordinated.[32] As one example of the confusion as to where terminal and bridging CO bands should occur, Song and co-workers[12] cite Rygh's paper[32] as evidence for bridging CO bands occurring in the mid-1900 cm^{-1} region even though Rygh concludes otherwise.

The 1942 cm^{-1} band is very small or nonexistent on CoRe(A). The presence of CO bands greater than 2100 cm^{-1} for CoRe(A), especially the high 2175 cm^{-1} band, points to the CoRe(A) catalyst having a greater quantity of higher oxidation state Co(I), Co(II), and Co(III) centers. The terminal Co(0)−CO band is shifted by 19 cm^{-1} lower wavenumbers for CoRe(N) as compared to CoRe(A). This indicates a stronger CO adsorption on CoRe(N) as compared to CoRe(A). This is also an indication of a larger cobalt cluster size for CoRe(N) compared to CoRe(A). Earlier IR studies[27] on the effect of cluster size on CO peak shifts suggest that as the cluster size decreases, the peak shifts from strongly bound surface species to less strongly bound surface species, i.e., CO adsorption is stronger on larger clusters. This result is consistent with the XRD results (Figures 2 and 3) where the CoRe(A) catalyst exists as particles with sizes less than about 2 nm. Since CoRe(A) is more selective toward oxygenates, it can be inferred that less strongly adsorbed carbonyls are involved in CO hydrogenation and oxygenate formation.

CO Adsorption at 230 °C. The results for CO adsorption for CoRe(N) and CoRe(A) at 230 °C are also shown in Figure 5. CO is adsorbed almost exclusively in the linear mode (2073 cm^{-1}) on CoRe(A). The amount of CO adsorbed on the Co(II)/Co(III) (2175 cm^{-1}) and Co(I) sites (2119 cm^{-1}) decreases at 230 °C compared to 25 °C, showing that CO is weakly bonded to these surface sites as expected from their higher CO frequencies.

For CoRe(N), the CO adsorption at 1942 cm^{-1} is reduced at 230 °C as compared to 25 °C. More linearly adsorbed CO sites are found in CoRe(N) than CoRe(A), which is consistent with the higher CO reaction rates on CoRe(N) compared to CoRe(A), as shown in Table 2. Similar results have been reported on Co/SiO_2 catalysts prepared using these same two precursors,[14,22] where the nitrate precursor catalysts (both promoted and unpromoted) were found to have higher rates of CO conversion than those prepared from an acetate precursor. Also, for CoRe(N) the CO peak at 2053 cm^{-1} (Figure 5) is more strongly adsorbed relative to the 2073 cm^{-1} peak for CoRe(A), which leads to higher selectivities for hydrocarbons. Similar conclusions were drawn for CO adsorption on Pd catalysts[27] where weakly adsorbed CO on small Pd crystallites was found to be responsible for higher methanol selectivity, while more strongly adsorbed CO was responsible for methane (hydrocarbon) selectivity.

It has been reported[5,38] that the probability of C−O bond dissociation depends mainly on the strength of the metal−carbon (M−C) bond. Strong M-C bonds are favored by electron-rich metal centers due to π-backbonding, which at the same time weakens the C≡O triple bond leading to lower carbonyl stretching frequencies. The lower the CO stretching frequency, the weaker the C−O π-bonds and the greater the rate of C−O bond cleavage and hydrogenation relative to CO insertion. This decreases selectivity toward oxygenates and favors the formation of hydrocarbons[38] because CO insertion is a key step in the proposed mechanism for C_2^+ oxygenates formation.[5] The higher C_2^+ oxygenates selectivity observed for the CoRe(A) catalyst (Table 2) corresponds to the presence of more weakly coordinated CO, consistent with these earlier results.

It is interesting that the TPR results showed a similar amount of reduced cobalt for both catalysts. The IR data is clearly indicating that the CoRe(A) catalyst has more surface-accessible Co in +1, +2, and +3 oxidation states. The larger particle size for the CoRe(N) catalyst means that the oxidized cobalt (+2/+3 oxidation states) present for that system is buried under a Co/Re shell and not available to either influence the surface cobalt centers or for coordinating CO. The ~2 nm CoRe(A) particles, on the other hand, have exposed Co(II)/Co(III) centers, probably in the form of Co_3O_4, that reduces the overall electron-density on the nearby surface Co(0) centers leading to higher CO stretching frequencies.

CO Hydrogenation at 230 °C for CoRe(N). The DRIFTS results for CO hydrogenation (flowing H_2 + He over catalyst preadsorbed with CO at 230 °C) for CoRe(N) is presented in Figure 6. These spectra are taken at different times after starting H_2 flow ($t = 0$ s).

On comparing the spectra at $t = 0$ and 28 s, the linearly adsorbed CO peak height is reduced but the lower energy band increases in a relative sense. This could indicate that some of the linearly adsorbed CO's are transforming to bridge-type sites

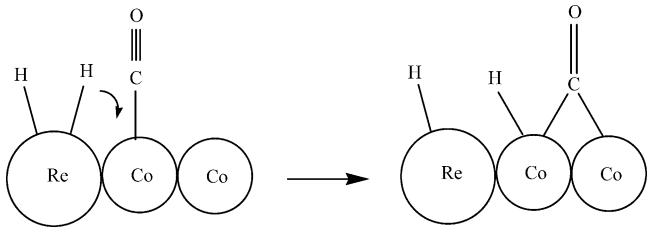

Figure 7. Proposed mechanism for transformation of linearly adsorbed CO to bridge-type.

under the flow of hydrogen. There could be three possibilities for CO hydrogenation in this case:

1. CO hydrogenation taking place on linearly adsorbed CO sites.

2. CO hydrogenation taking place on bridge-type adsorbed CO sites.

3. CO hydrogenation taking place on both types of sites.

On the basis of these results, it cannot be concluded which of the three possibilities applies for CO hydrogenation for the CoRe(N) catalyst. CO hydrogenation activities of linear and bridged-type sites are not fully understood. Bridging CO's have been found to react more readily with hydrogen than the linearly adsorbed CO on promoted cobalt catalysts similar to those reported here.[8,9] It has also been reported[8] that a low density of bridging carbonyls results in a low chain growth probability and low C_{5+} hydrocarbon selectivity. However, Song et al.[12] found that both linear and bridging CO's were equally reactive on an unpromoted Co/SiO_2 catalyst at reaction conditions comparable to those studied here.

What does appear clear is that lower CO stretching frequencies (bridging or terminal) on cobalt promote CO hydrogenation to form hydrocarbon products. Re is important here in helping to activate H_2 and allow it to readily migrate to the Co centers. For the CoRe(N) catalyst the lower wavenumber bands (1990−1920 cm^{-1}) could indicate that linearly coordinated CO is transforming to a doubly bridging mode on the Co surface and hydrogenation is taking place on these sites (case 2). A possible site transformation mechanism is presented in Figure 7. The spillover of hydrogen from Re to Co causes the linearly adsorbed CO to shift to a neighboring cobalt atom forming a bridge-type structure, which then undergoes hydrogenation.

CO Hydrogenation at 230 °C for CoRe(A). The DRIFTS results for CO hydrogenation for CoRe(A) are presented in Figure 8. This series of spectra is quite different from that seen for CoRe(N) in Figure 6. The 2183 cm^{-1} high frequency band associated with Co(II)/Co(III)−CO coordination is lost fairly quickly most likely due to reduction to Co(0) sites.

The site transformation from linear to bridged is not observed for CoRe(A). One possible explanation for this could be because of highly dispersed cobalt clusters, the possibility of having a neighboring cobalt atom is low. In other words, the presence of a Co−Co type structure is negligible. This also indicates that Re and Co exist in close proximity to each other, which agrees with the TPR results.

For CoRe(A) there is little doubt that the Co−CO linear sites are the active sites for CO hydrogenation. The shift in the CO peak (2074 cm^{-1} → 2047 cm^{-1}) probably reflects, in part, reduction of the electron-deficient Co(I), Co(II), and Co(III) sites producing a somewhat more electron-rich Co(0) surface, but still electron-deficient enough to favor oxygenate production. Lower CO surface coverage, as discussed previously, can also account for the shifting of CO stretching frequencies to lower wavenumbers.

Comparison of CO Adsorption for CoRe(N) and CoRe(A) at Different Temperatures. A comparison of CO adsorption for CoRe(N) at 25, 230, and 270 °C is presented in Figure 9. The peak shifts toward lower wavenumbers (red shift) with increasing temperature. This indicates that only strongly adsorbed surface species remain on the surface with increasing temperature, as expected. Also, the amount of linearly adsorbed CO is higher at 230 °C as compared to 25 °C and decreases with further increase in temperature to 270 °C, which shows an activated chemisorptions phenomenon. The peak at 1943 cm^{-1} is clearly seen at 25 °C but decreases in intensity as the temperature increases. This is curious since this band is assigned to either a bridging CO or a terminal carbonyl on a more electron-rich metal center. Neither should be lost more readily than a terminal Co(0)−CO.

A comparison of CO adsorptions for CoRe(A) is also presented in Figure 9. The red shift of the primary 2076 cm^{-1} band is similar with increasing temperature to that found in CoRe(N). The 2175−2180 cm^{-1} band associated with Co(II)/Co(III) sites persists at 230 °C but disappears at 270 °C. These

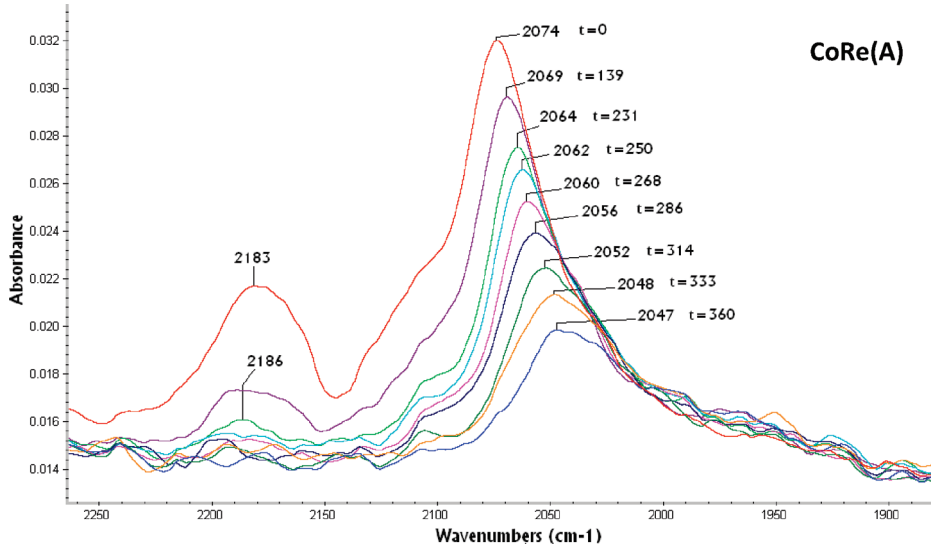

Figure 8. FTIR spectra for CO hydrogenation at 230 °C and 1 atm pressure for CoRe(A) at different times (in seconds) after starting H_2 flow (t = 0 corresponds to when H_2 flow started).

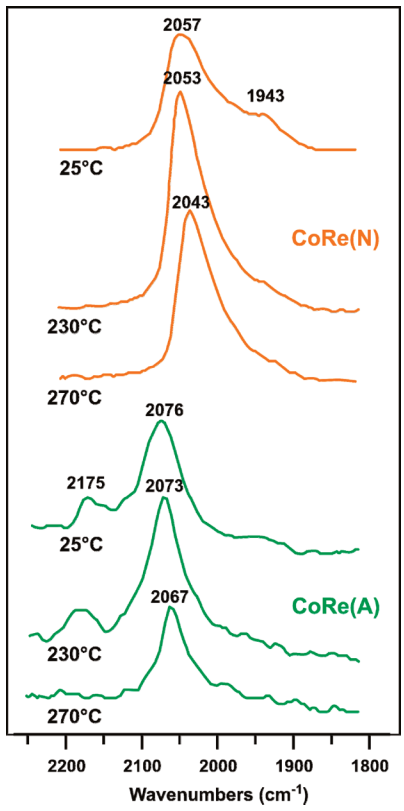

Figure 9. FT-IR spectra for CO adsorption for CoRe(N) and CoRe(A) at different temperatures and 1 atm followed by helium flushing for 7 min. The intensity of the CoRe(A) spectra have been increased relative to the CoRe(N) spectra to more clearly show the band structure.

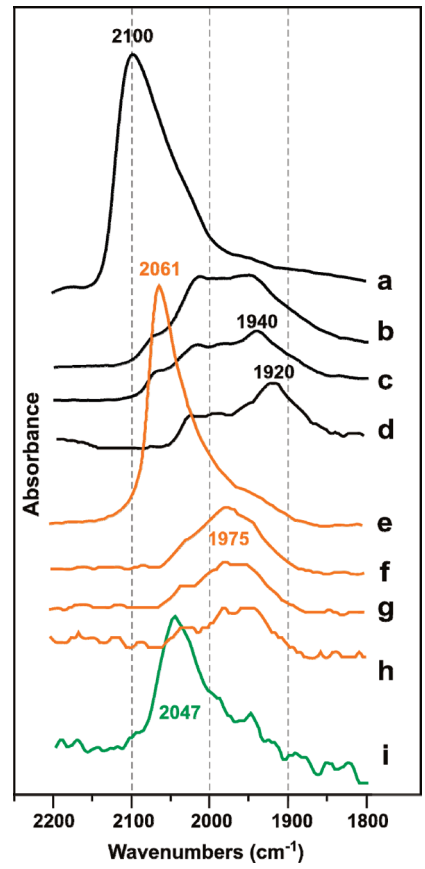

Figure 10. (a) Rygh's[1] FT-IR spectra at 250 °C immediately before H_2 addition; (b) after 35 min of H_2 exposure; (c) after 18 h followed by evaculation; (d) proposed Re−CO bands from CO only study; (e) CoRe(N) CO-only spectrum at 230 °C; (f) 111 s of H_2; (g) 129 s of H_2; (h) 397 s of H_2 (vertically expanded); (i) CoRe(A) catalyst after 360 s of H_2.

higher oxidation sites should be gradually reduced by CO and eventually disappear. The Co(I)−CO band proposed to be at 2125 cm^{-1} is found to reduce in intensity with increasing temperature, consistent with the weaker cobalt carbonyl bonding.

Comparison with Co/Re/γ-Al_2O_3 Fischer−Tropsch Catalyst. Figure 10 shows a comparison of the DRIFTS spectra under CO and H_2/CO conditions for CoRe(N), CoRe(A), and the 12% Co/1% Re/γ-Al_2O_3 Fischer−Tropsch catalyst system studied by Rygh and Nielsen.[1] Although there are certainly some differences in exact band positions between Rygh's catalyst system and CoRe(N), there are a number of similarities. The fact that CoRe(N) functions mainly like a Fischer−Tropsch catalyst fits with the spectral analogies to Rygh's catalyst. It is clear that the CoRe(A) catalyst, however, is quite different in that it lacks most of the lower frequency CO bands associated with Fischer−Tropsch activity.

Rygh has assigned a series of broad CO bands between 2020 and 1920 cm^{-1} (Figure 10d) as arising from linear Re carbonyls. This could be responsible for or contribute to the 1943 cm^{-1} shoulder seen for the CoRe(N) catalyst. Re is less electronegative relative to Co, the Re 5d orbitals overlap better with the CO π*-antibonding orbitals, so Re should engage in more π-backbonding to a terminal carbonyl, leading to lower CO stretching frequency. The presence of larger Re clusters, which are likely on the larger CoRe(N) catalyst particles could lead to these types of Re−CO bands. The lack of them in the CoRe(A) catalyst is, once again, generally consistent with the smaller particle size and more atomically dispersed Re centers.

The proposed larger and more isolated Re clusters on the CoRe(N) catalyst are consistent with the TPR results, where a shoulder is observed for the case of CoRe(N) catalyst. This shoulder is likely due to reduction of rhenium oxide and cobalt oxide in contact with each other. The peak observed after the shoulder would then be due to the slower reduction of cobalt oxide not in contact with Re. This is not observed for the CoRe(A) catalyst due to the more highly dispersed Re and much smaller Re(0) clusters that result.

CO Desorption Rate. CO desorption rates were calculated for CoRe(N) based on decrease in peak height with respect to time. The results for 230 and 270 °C are presented in Figures 11 and 12, respectively.

The surface CO desorption rate is faster in the presence of hydrogen than that of helium at both temperatures. This result is expected, as CO adsorbed on the surface depletes faster because of hydrogenation reactions at these temperatures. A comparison of Figures 11 and 12 shows that the CO desorption rate is faster at higher temperatures, for both helium and hydrogen flow conditions, which is also an expected result.

Conclusions

Experimental results showed significant differences in catalyst behavior and physical properties for two nominally identical Re-promoted cobalt catalysts prepared from cobalt nitrate [CoRe(N)] and cobalt acetate [CoRe(A)] precursors. XRD showed no peaks for the CoRe(A) catalyst, indicating that cobalt is present in clusters less than 2 nm in size. CO hydrogenation activity/selectivity results on these two catalysts showed that while the rate of CO reaction on CoRe(N) was greater than CoRe(A), the selectivities toward ethanol and oxygenates were far higher for the CoRe(A) catalyst. This appears to be due in

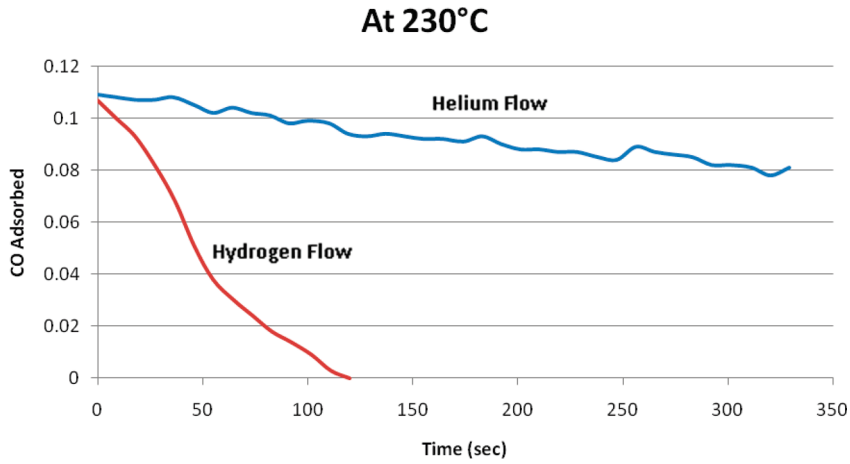

Figure 11. CO desorption rates for CoRe(N) at 230 °C and 1 atm pressure during helium and hydrogen flow.

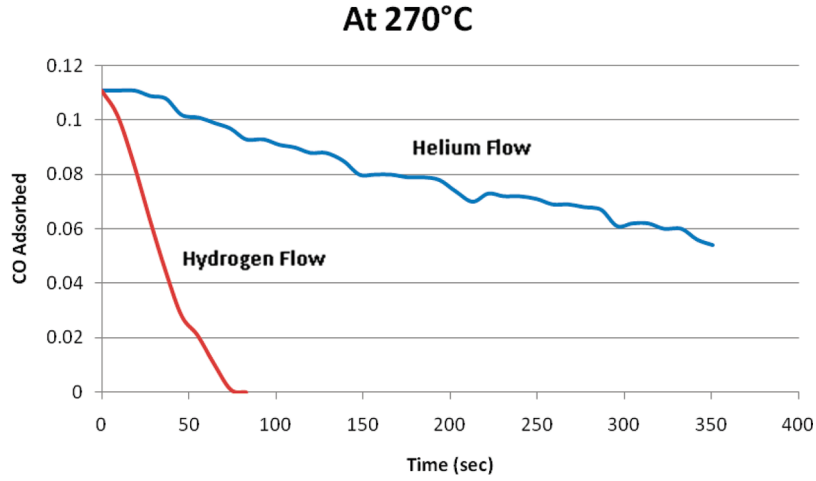

Figure 12. CO desorption rates for CoRe(N) at 270 °C and 1 atm pressure during helium and hydrogen flow.

part to the smaller cluster size of highly dispersed cobalt and rhenium phases for CoRe(A).

FT-IR DRIFTS studies demonstrate considerably different metal carbonyl coordination sites for both catalysts. The CoRe(N) catalyst system showed carbonyl bands with lower stretching frequencies (2057 cm^{-1}) relative to CoRe(A) and distinct similarities to $Co/Re/Al_2O_3$ Fischer−Tropsch catalysts characterized by Rygh and Nielsen.[1] The CoRe(A) catalyst, in marked contrast, had a higher frequency band assigned to Co(0)−CO (2074 cm^{-1}) and extremely high frequency bands at 2175−2183 cm^{-1}, assigned to Co(II)/Co(III)−CO (due to Co_3O_4), and 2125 cm^{-1} assigned to Co(I)−CO resulting from CO (or H_2) reduction of the Co(II)/Co(III) centers. Although carbonyl bands around 1950 cm^{-1} were found on CoRe(N), which could be assigned to either bridging CO's or terminal Re carbonyls, few such sites were found on CoRe(A). CO hydrogenation results for CoRe(N) demonstrate that lower frequency carbonyls undergo hydrogenation to form far more hydrocarbon products, in analogy with related Fischer−Tropsch systems. For CoRe(A) the linear sites are found to be the active sites for CO hydrogenation and production of higher amounts of desired oxygenated products. A stronger interaction of CO with the surface was observed for CoRe(N) compared to CoRe(A) at all temperatures, which is an indication of larger cobalt cluster size. Sites on CoRe(A) that adsorb CO linearly and relatively weakly (i.e., higher CO stretching frequencies) are responsible for higher selectivity toward oxygenates. Red shifts of linearly adsorbed CO peaks were observed for both the catalysts with increasing temperature.

The differences in catalyst behavior between CoRe(N) and CoRe(A) are tied into the electronic differences indicated by the metal carbonyl FT-IR spectra. The more electron-rich bulk-like Co and Re centers in the CoRe(N) catalyst causes it to behave more like a traditional Fischer−Tropsch catalyst system. The larger particle size of the CoRe(N) catalyst has the oxidized Co_3O_4 crystallites buried beneath the Co/Re metallic surface, since any significant amounts of exposed Co_3O_4 would coordinate CO and produce higher frequency carbonyl bands, which are not observed. The 1942 cm^{-1} band for CoRe(N) (and general band intensity between 2000 and 1900 cm^{-1}) can be tentatively assigned to bridged CO on cobalt and terminal Re-CO's. The Re−CO bands, if present, indicate larger clusters of Re on the surface.

In marked contrast, the CoRe(A) catalyst has very small ~2 nm sized particles with exposed Co_3O_4 and more atomically dispersed Co(0) and Re(0) centers. The higher Co(0)−CO stretching frequency arises from the smaller Co cluster size and presence of nearby Co_3O_4 species that are electron-withdrawing and reduce the electron-density on the Co(0) centers. If the observation of Re(0) cluster linear carbonyls in the 2000−1920 cm^{-1} region is correct for the CoRe(N) catalyst system, the lack of bands in this region for CoRe(A) indicates that the more atomically dispersed Re centers may not be as effective in activating H_2 and providing H atoms to the Co sites. The presence of surface accessible Co_3O_4 on the CoRe(A) catalyst indicates that H_2 reduction is more difficult than we anticipated, providing support for the lack of significantly sized Re clusters.

The selectivity of the CoRe(A) catalyst for oxygenates appears to be clearly tied into its lower hydrogenation activity. The current results indicate that it may be possible to maintain the oxygenate selectivity while increasing the overall catalyst activity for CoRe(A) by increasing the amount of Re used and experimenting with longer H_2 catalyst reduction conditions. Maintaining nanosized catalyst particles and highly dispersed Re (or other H_2-activating metal) appears to be a critical feature for oxygenate selectivity based on this study.

Acknowledgment. The authors are thankful to Center for Nanophase Material Sciences, which is sponsored at Oak Ridge National Laboratory by the division of Scientific User Facilities, U.S. Department of Energy. The funding from Chevron Energy Technology Company is gratefully acknowledged.

References and Notes

(1) Rygh, L. E. S.; Nielsen, C. J. *J. Catal.* **2000**, *194*, 401.
(2) Walter, A.; Rosillo-Calle, F.; Dolzan, P.; Piacente, E.; Borges da Cunha, K. *Biomass Bioenergy* **2008**, *32*, 730.
(3) Prasad, S.; Singh, A.; Joshi, H. C. *Resour., Conserv. Recycl.* **2007**, *50*, 1.
(4) Subramani, V.; Gangwal, S. K. *Energy Fuels* **2008**, *22*, 814.
(5) Spivey, J. J. A. E. *Chem. Soc. Rev.* **2007**, *36*, 1514.
(6) Kababji, A.; Joseph, B.; Wolan, J. *Catal. Lett.* **2009**, *130*, 72.
(7) Kadinov, G.; Bonev, C.; Todorova, S.; Palazov, A. *J. Chem. Soc.—Faraday Trans.* **1998**, *94*, 3027.
(8) Tsubaki, N.; Sun, S.; Fujimoto, K. *J. Catal.* **2001**, *199*, 236.
(9) Jiang, M.; Koizumi, N.; Ozaki, T.; Yamada, M. *Appl. Catal. A: Gen.* **2001**, *209*, 59.
(10) F. P. Larkins, M. J. R. *J. Mol. Catal.* **1991**, *5*, 233.
(11) Fredriksen, G. R.; Blekkan, E. A.; Schanke, D.; Holmen, A. *Chem. Eng. Technol.* **1995**, *18*, 125.
(12) Song, D.; Li, J.; Cai, Q. *J. Phys. Chem. C* **2007**, *111*, 18970.
(13) Heal, M. J.; Leisegang, E. C.; Torrington, R. G. *J. Catal.* **1978**, *51*, 314.
(14) Matsuzaki, T.; Takeuchi, K.; Hanaoka, T.-a.; Arawaka, H.; Sugi, Y. *Appl. Catal. A: Gen.* **1993**, *105*, 159.
(15) Takehiko Matsuzaki, K. T.; Taka-aki, H.; Hironori, A.; Yoshihiro, S. *J. Jpn. Petrol. Inst.* **1994**, *37*, 179.
(16) Vada, S.; Hoff, A.; ÅdnaneS, E.; Schanke, D.; Holmen, A. *Top. Catal.* **1995**, *2*, 155.
(17) Hong, J.; Chu, W.; Chernavskii, P. A.; Khodakov, A. Y. *Appl. Catal. A: Gen.* **2010**, *382*, 28.
(18) Feller, A. M. c.; van Steen, E. *J. Catal.* **1999**, *185*, 120.
(19) Moradi, G. R.; Basir, M. M.; Taeb, A.; Kiennemann, A. *Catal. Commun.* **2003**, *4*, 27.
(20) Khodakov, A. Y.; Chu, W.; Fongarland, P. *Chem. Rev.* **2007**, *107*, 1692.
(21) Niemelä, M. K.; Krause, A. O. I.; Vaara, T.; Kiviaho, J. J.; Reinikainen, M. K. O. *Appl. Catal. A: Gen.* **1996**, *147*, 325.
(22) Matsuzaki, T. T., K.; Hanaoka, T.; Arakawa, H.; Sugi, Y. *Trans. Mater. Res. Soc. Jpn.* **1994**, *18A*, 417.
(23) Hilmen, A. M.; Schanke, D.; Hanssen, K. F.; Holmen, A. *Appl. Catal. A: Gen.* **1999**, *186*, 169.
(24) Hilmen, A. M.; Schanke, D.; Holmen, A. *Catal. Lett.* **1996**, *38*, 143.
(25) Das, T. K.; Jacobs, G.; Patterson, P. M.; Conner, W. A.; Li, J.; Davis, B. H. *Fuel* **2003**, *82*, 805.
(26) Martínez, A.; López, C.; Márquez, F.; Díaz, I. *J. Catal.* **2003**, *220*, 486.
(27) Fajula, F.; Anthony, R. G.; Lunsford, J. H. *J. Catal.* **1982**, *73*, 237.
(28) Busca, G.; Guidetti, R.; Lorenzelli, V. *J. Chem. Soc., Faraday Trans.* **1990**, *86*, 989.
(29) Bhargava, S. K.; Akolekar, D. B. *J. Colloid Interface Sci.* **2005**, *281*, 171.
(30) Hoffmann, F. M. *Surf. Sci. Rep.* **1983**, *3*, 107.
(31) Zhang, J.; Chen, J.; Ren, J.; Sun, Y. *Appl. Catal. A: Gen.* **2003**, *243*, 121.
(32) Rygh, L. E. S.; Ellestad, O. H.; Klaeboe, P.; Nielsen, C. J. *Phys. Chem. Chem. Phys.* **2000**, *2*, 1835.
(33) Dees, M. J.; Shido, T.; Iwasawa, Y.; Ponec, V. *J. Catal.* **1990**, *124*, 530.
(34) Laneman, S. A.; Fronczek, F. R.; Stanley, G. G. *Inorg. Chem.* **1989**, *28*, 1206.
(35) Ray, L.; Sweany, T. L. B. *Inorg. Chem.* **1977**, *16*, 415.
(36) Cirjak, L. M.; Huang, J.-S.; Zhu, Z.-H.; Dahl, L. F. *J. Am. Chem. Soc.* **1980**, *102*, 6623.
(37) Takeuchi, K.; Hanaoka, T.-a.; Matsuzaki, T.; Sugi, Y.; Ogasawara, S.; Abe, Y.; Misono, T. *Catal. Today* **1994**, *20*, 423.
(38) Golodets, G. I.; Ilchenko, N. I.; Shmyrko, Y. I. *React. Kinet. Catal. Lett.* **1989**, *39*, 169.

JP104878E